

Catalysts for the production of styrene from ethylbenzene: redox and deactivation study

O. Irún, S.-A. Sadosche, J. Lasobras, J. Soler*, E. Francés, J. Herguido and M. Menéndez

*Catalysis, Molecular Separations and Reactor Engineering Group (CREG)
Aragon Institute for Engineering Research (I3A), University of Zaragoza, 50009 Zaragoza,
Spain*

**corresponding author. Tel: +34876555481; fax: +34976762142. E-mail address:
jsoler@unizar.es*

Abstract

In this work, a pulse plant has been used to study the redox properties, activity and coke generation of four catalysts in ethylbenzene dehydrogenation to produce styrene. CO₂ was used as weak oxidant. A physicochemical and structural characterization was carried out in order to verify possible changes in the catalysts after the tests. The experiments consisted of a reduction test with H₂, oxidation with CO₂, reaction with ethylbenzene, regeneration with CO₂ and coke combustion and reoxidation with O₂. These experiments were carried out at three temperatures (450, 500 and 550 °C). With the catalyst that exhibited the best results, MnO₂-ZrO₂, additional experiments with different oxidation states were carried out in order to determine the influence on its activity and redox properties to assess the feasibility of using CO₂ as a regenerating agent during the ethylbenzene dehydrogenation reaction.

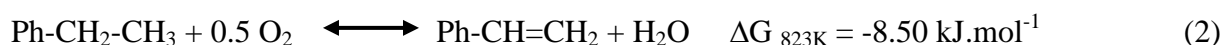
Keywords: Ethylbenzene, Styrene, Dehydrogenation, Carbon dioxide.

1. Introduction

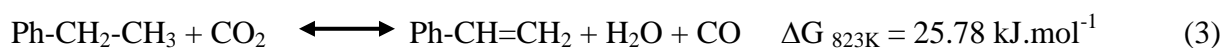
Styrene production by oxidative dehydrogenation in presence of CO₂ has been studied in a significant number of recent works. The reason for such interest is related with the difficulties associated with the currently employed process of styrene production by catalytic dehydrogenation of ethylbenzene: a) the reaction is highly endothermic (1) and b) a large volume of steam in the feed to avoid catalyst deactivation by coke is required. This interest is also a consequence of the large quantities of styrene produced worldwide, given that it is among the ten main base chemical products. Several production procedures have been proposed as alternatives to that currently employed in industry [1].



Oxidative dehydrogenation is considered as a promising alternative since the removal of hydrogen by the formation of water converts the global reaction to an exothermic and irreversible one (2).



Unfortunately, as is often found in oxidative dehydrogenation, the formation of carbon oxides appears as an undesired reaction, decreasing the selectivity to olefins. Oxidative dehydrogenation with CO₂ has appeared as an alternative to oxidative dehydrogenation with avoiding the problem of total combustion of the hydrocarbons (3).



Although CO₂ has historically been considered as an inert gas, many recent reports show that it can act as a weak oxidant in reactions such as methane coupling, oxidative dehydrogenation of C₂-C₄ alkanes, oxidative dehydrogenation of alkylbenzene, or aromatization of lower alkanes to benzene, as reviewed by Wang and Zhu [2]. In the oxidation of butane to maleic anhydride, the improvement in selectivity due to the presence of CO₂ has been explained by an increase in the oxidation degree of the catalyst [3]. Focusing on the oxidative dehydrogenation of ethylbenzene,

a large variety of catalysts has been tested. Most of them include Fe, V or Cr oxides as active component ([4] and references therein), although supported Mn oxides [5], Sn oxides [6] and Ga oxides [7] have also been employed.

A question that has not been fully solved is the actuation mechanism of CO₂ in the oxidative dehydrogenation reaction. The high performance of catalyst containing vanadium oxides has been explained by a redox mechanism, specifically the Mars-van Krevelen mechanism [8,9]. Araujo et al. [10] found a Fe⁺²-Fe⁺³ redox cycle in FeCrO_x catalysts, similar to the mechanism proposed by Atanda et al. [11] and Balasamy et al. [12,13]. Sugino et al. [14] suggested an oxidative dehydrogenation mechanism. Another factor contributing to the catalyst stability in the presence of CO₂ is the coke formation [15]. Krylov et al. [16] observed that heavy hydrocarbons are subject mainly to oxidative cracking upon interaction with CO₂ over manganese oxide catalysts.

Several catalysts found to be active and selective in literature, which were synthesised and characterized, have been tested using transient studies in a reactor with pulses of either H₂, ethylbenzene, CO₂ or O₂:

(i) Vanadium oxides are frequently used for ethylbenzene dehydrogenation with CO₂. In the literature, several supports have been tested including active carbon [17], alumina [18-22] and mesoporous materials [23]. Moreover, antimony [18, 20] has been proposed as additive.

(ii) Zirconium oxides have been used in combination with other oxides, i.e. MnO₂ [5], SnO₂ [6] and TiO₂ [24] for ethylbenzene dehydrogenation at temperatures between 550 and 600 °C with high selectivities to styrene.

(iii) Vanadium-doped titanium mixed oxides (V-TiO₂) were used by Li et al. [25]. These authors proposed a sol-gel method to synthesise the catalysts in order to achieve high vanadium dispersion and, after studying the effect of vanadium loading between 1 and 9 mol% on the catalytic performance, they obtained a maximum value with 6 mol% and high styrene selectivity.

(iv) $\text{TiO}_2\text{-ZrO}_2$ mixed oxides, used as a support, give high specific surface area, good redox properties and high thermal and mechanical stability. Vanadium oxides provide the catalytic activity for the reaction and CeO_2 is well-known as oxygen storage/ release material. Thus the combination of both vanadium and cerium was expected to achieve an improvement in the performance of the catalyst. Reddy et al. [4, 26] studied the feasibility of the use of $\text{V}_2\text{O}_5\text{-CeO}_2/\text{TiO}_2\text{-ZrO}_2$ catalyst for the reaction.

The objective of these experiments was to assess the capability of the catalyst to be reduced by H_2 and then to be oxidized with CO_2 (i.e. to evaluate the redox capability of the catalyst) and also the effect of CO_2 on a catalyst after being employed in ethylbenzene dehydrogenation. The experimental results and the effect of the operating conditions are described and discussed, and the consequences of these results considered in relation to the role of CO_2 in the reaction will be proposed. In addition, these experiments will provide preliminary information to assess the feasibility of using a two-zone fluidized bed reactor [27] as a contacting device to counteract the catalyst deactivation by including a second zone where the catalyst is regenerated with CO_2 .

2. Experimental

2.1. Catalyst selection and preparation

After reviewing the literature, the four different catalysts described below were selected from those with the better reported performances. They were synthesized following the authors' recommended procedures.

(i) In accordance with the procedure described by Chen et al. [21], $\text{V}_2\text{O}_5/\text{Al}_2\text{O}_3$ (1.5 mmol V/g catalyst) was prepared using an incipient wetness impregnation of $\gamma\text{-Al}_2\text{O}_3$ with NH_4VO_3 dissolved in an aqueous solution of oxalic acid during 24 hours. Later, the catalyst was dried at $120\text{ }^\circ\text{C}$ for 4 hours and calcined in air at $550\text{ }^\circ\text{C}$ during a further 4 hours more.

(ii) Burri et al. [5] proposed a $\text{MnO}_2\text{-ZrO}_2$ binary oxide catalytic system for the effective utilization of CO_2 as an oxidant in the ethylbenzene dehydrogenation to styrene monomer. This catalyst exhibited a conversion of 73% with a selectivity of 98% at 650 °C. The recommended method to prepare $\text{MnO}_2\text{-ZrO}_2$ oxides with 10 mol% MnO_2 (0.84 mmol Mn/ g catalyst) was coprecipitation. Zirconyl nitrate and manganese nitrate were selected as precursors (stirred at room temperature for 0.5 hours) and aqueous ammonia solution was used as a hydrolyzing agent (added until the pH of the solution reached 9). After stirring for 1 hour, the solution was aged for 12 hours at 100 °C in an oven. The precipitate obtained was filtered under vacuum conditions and washed with distilled water. The solid was dried at 120 °C for 12 hours and calcined at 550 °C for 6 hours in a muffle furnace.

(iii) According to Li et al. [25], the synthesis method of V-TiO₂ (1.25 mmol V/g catalyst) consists of several steps. First of all, titanium isopropoxide ($\text{Ti}(\text{OiPr})_4$) was dissolved in ethanol to form Ti sol after which acetylacetonone was added as chelating agent. Ammonium metavanadate (NH_4VO_3) was dissolved in 0.25 M oxalic acid and this solution slowly poured into the Ti sol and continuously stirred until the sol turns into a gel. After 7 days aging, the resulting dried gel was calcined in a muffle furnace at 550 °C during 4 hours.

(iv) Reddy et al. [4, 26] synthesised $\text{V}_2\text{O}_5\text{-CeO}_2/\text{TiO}_2\text{-ZrO}_2$ with several $\text{TiO}_2\text{:ZrO}_2$ ratios. The optimum composition was $\text{TiO}_2\text{-ZrO}_2$ (1:1 molar ratio), $\text{CeO}_2\text{-ZrO}_2$ (7.5 wt.% + 7.5 wt.%) and 0.84 mmol V/g catalyst. $\text{TiO}_2\text{-ZrO}_2$ support was prepared using a coprecipitation method from TiCl_4 and ZrOCl_2 aqueous solutions by hydrolysis with ammonium hydroxide. Precursors were added under stirring until the pH reaches a value between 7 and 8. Later, the solution was aged hydrothermally during 12 hours at 100 °C and then the precipitate was filtered under pressure and washed with deionized water. The obtained cake was dried at 120 °C and finally calcined at 550 °C for 6 hours in a muffle furnace. The solid obtained was used as a support and an amount of CeO_2 (7.5 wt %) and V_2O_5 (7.5 wt %) was calculated to be deposited over the support by

means of standard wet impregnation. The precursors used were ammonium metavanadate (NH_4VO_3) and ceria ammonium nitrate ($\text{CeH}_8\text{N}_8\text{O}_{18}$) which were dissolved in deionized water. The support was added under stirring. The excess water was removed by heating at 120 °C for 12 hours. Finally, the solid obtained was calcined during 6 hours at 550 °C in a muffle furnace.

2.2. Catalyst characterization

The samples were characterized after completing all the steps of the transient study at every temperature.

Specific BET surface areas of fresh samples and samples after reaction were obtained by static N_2 adsorption measurements using TriStar 3000 (V6.08 A) equipment on previously degassed samples. The degasification was carried out in two stages: the first at a heating rate of 10 °C min^{-1} until 90 °C, maintaining this temperature during 1h, and the second at a heating rate of 10 °C min^{-1} until 200 °C, maintaining the temperature for 8 h.

XRD patterns were obtained using a Rigaku/Max System diffractometer Cu (Model D/max 2500) equipped with a graphite monochromator. The step size was 0.03° with 2θ scanning from 5° to 80°.

In order to know the redox capacity of the catalysts, the activity and distribution of the products in reaction, and the coke formation and regeneration, a pulse plant was designed and built (Figure 1). This plant consists of four mass flow controllers (Alicat Scientific) to introduce the necessary gases into the system. Two helium controllers (one for the carrier and the other for diluting the other gases or sweeping the ethylbenzene at a partial pressure according to the temperature of the liquid), a hydrogen controller and an oxygen or CO_2 controller are used, and the flow changed by means of several valves operated manually. The ethylbenzene is located in two saturators arranged in series and placed in two water recipients at a controlled temperature. The injection of the reactant pulses is carried out by means of a six way microelectric valve (Valco Instruments Co. Inc.) with a loop of 1 mL capacity that is released in a helium carrier

flow to reach the catalyst located in a quartz reactor placed in an electric oven. The reactant flow can also be fed continuously by using a four way microelectric valve (Valco Instruments Co. Inc.). In order to compare the results of every pulse with the signal of the same reactant without reaction, a similar reactor with an inert solid and the same amount of catalyst powder in the reactor where the reaction takes place is arranged in parallel. Thus, at the end of every sequence of pulses passing reactant through the catalyst, another sequence can be sent (5 pulses) without reaction in order to calculate the conversion of the reactant by comparison of the areas in both series of pulses. The outlet gases are analyzed continuously by mass spectroscopy using Prolab Thermo Onix equipment with Thermo Gas Works software. The mass flow of the gases, oven temperature control and movement of the microelectric valves are programmed, controlled and registered by a PC with homemade software made using the Labview program. The methodology for each experiment consisted of loading 500 mg of catalyst into the reactor with a particle size range between 160-320 μm . The sample was heated at 5°C min^{-1} under helium flow up to the characterization temperature (450, 500 or 550 $^\circ\text{C}$). The reduction step consisted of 50 pulses of hydrogen (50 %) with a frequency of 1 minute. After 10 minutes of purging, the oxidation with CO_2 was carried out by injecting 25 pulses of CO_2 (50%). After a further 10 minutes of purging, the ethylbenzene reaction took place. In this case several experiments were carried out in which the partial pressure was modified (2.44% and 5.05%) to study the influence of the ethylbenzene concentration supplied. In each experiment 25 pulses were injected. The subsequent regeneration step (reoxidation with CO_2) consisted of 10 pulses CO_2 (50%). Finally, in order to remove all the remaining coke and to oxidize the catalyst completely, 50 pulses of O_2 (50%) were injected. Data analysis was carried out using Origin software in order to calculate the peak areas of each pulse.

3. Results and discussion

3.1. Catalyst characterization

Table 1 shows the BET surface area of the four catalysts before and after every experiment for verification of the textural changes that take place during both the redox and reaction experiments. It can be seen that V_2O_5/Al_2O_3 catalyst has a higher surface area than the others, but this reduces after use. Chen et al. [21] suggest there is significant coke deposition that cannot be alleviated by CO_2 . So, for this catalyst, coke is exclusively removed in the oxidation with oxygen step. This fact can produce a sintering process due to the high temperature occurring during the combustion of the coke that, as a result, produces a decrease in the BET surface area. However, for the other catalysts, the loss of BET surface is lower. This can also be explained by coke formation and later combustion that hardly cause sinterization. Moreover, Burri et al. [5] demonstrated that MnO_2-ZrO_2 deactivation by coke deposition was lower than for other kinds of catalyst and that CO_2 pretreatment clearly decreased the deactivation by coke formation.

XRD patterns of fresh and used catalyst are shown in order to both check the crystallinity of the samples and verify any possible structural change during the experiments. Fig 2a shows the presence of peaks corresponding to γ -alumina ($2\theta = 36, 46$ and 66°) and a weak peak at $2\theta = 21^\circ$ suggesting that VO_x species are highly dispersed on the alumina surface and that no sinterization takes place during the experiments. XRD spectra for the MnO_2-ZrO_2 samples (Fig 2b) show the presence of peaks corresponding to MnO_2 crystals ($2\theta = 27, 32, 48$ and 58°) and ZrO_2 ($2\theta = 21, 25$ and 38°) while mixed oxides are amorphous or poorly crystalline (with a broad and weak peak between $2\theta = 25-35^\circ$ [5]). No changes were noticed after the use of the catalyst. In Fig 2c, peaks associated with titanium crystals are present, i.e. for titanium oxide. The presence of anatase ($2\theta = 22, 35, 41, 53, 54, 62, 68, 70$ and 75°) and rutile ($2\theta = 24^\circ$) was detected, but not for V_2O_5 , which implies a good vanadium dispersion. Finally, in Fig. 2d, the spectra show a small degree of crystallinity, consistent with the results of Reddy et al. [4], but other Ce and Zr species are also present: $ZrTiO_4$ (broad and weak peak between $2\theta = 15-36^\circ$); ZrV_2O_7 ($2\theta = 14, 20$ and 28°) and $CeVO_4$ ($2\theta = 21, 27,$ and 45°).

3.2. Transient study

The results were obtained of sending pulses of hydrogen, CO₂, ethylbenzene and oxygen at three temperatures (450, 500 and 550 °C) with the four catalysts studied. In Figure 3a a comparison of the catalysts at 550 °C during the reduction step with hydrogen is shown. H₂O could not be quantified due to the low sensitivity for mass spectrometer for the lower masses. It can be seen that hydrogen conversion in the first pulses is higher for MnO₂-ZrO₂. However, V-TiO₂ reduction is very slow. This behaviour is in accordance with results obtained by Dinse et al. [28] who observed the influence of both support and temperature in the vanadium catalysts reducibility. Figure 3b shows a comparison of the reduction capacity of the four catalysts at the three temperatures. The presence of Ce can provide a better reduction capacity for the V₂O₅-CeO₂/TiO₂-ZrO₂ at all the temperatures studied, in contrast with the other vanadium based catalysts. This is consistent with the well-known oxygen storage/release capacity of ceria owing to oxygen vacancies in the catalyst [29, 30].

In Figure 4 the treatment with CO₂ is presented. It can be observed that MnO₂-ZrO₂ is the catalyst that exhibits a higher CO₂ consumption. This is a consequence of ZrO₂ crystallographic phases that contribute towards a good activation of CO₂ [31] and MnO₂ (oxide of moderate basicity) participating in a redox process with CO₂ reduction [16]. CO was detected during this step and the quantity of consumed CO₂ is consistent with CO that appears, which proves that CO₂ is consumed by active metal oxidation.

Figure 5 presents the results of the ethylbenzene reaction with a partial pressure of 2.44%. It was observed that selectivity to styrene was almost 100% in all cases. In Figure 5a, the conversion of ethylbenzene for the catalysts studied at 550 °C is shown. It can be seen that V₂O₅/Al₂O₃ and V-TiO₂ exhibited high activity in the first pulses but, after 15 pulses, a sharp deactivation took place due to two possible effects: removal of lattice oxygen of the catalyst and coke deposition. This is consistent with the behaviour observed by other authors [21, 25]. The

addition of CeO_2 to $\text{V}_2\text{O}_5/\text{TiO}_2\text{-ZrO}_2$ prevented catalyst deactivation, as evidenced in the literature [4], but the conversion was lower. However, $\text{MnO}_2\text{-ZrO}_2$ exhibited both high conversion and low deactivation. Figure 5b shows the influence of the temperature on the conversion of ethylbenzene for the best catalyst ($\text{MnO}_2\text{-ZrO}_2$). As would be expected, the higher the temperature the greater the quantity of ethylbenzene that is converted into products. At temperatures of 500 °C and 550 °C, the catalyst remains activated during the 25 pulses sent with only a slight drop, suggesting that lattice oxygen or coke formation are not limitations for the reaction in the range of time-on-stream studied. However, at 450 °C the reduction in conversion is more marked. This can be due to lower oxidation by CO_2 , as shown in Figure 4, and to the fact that the manganese of the catalyst is not in an appropriate oxidation state to carry out the reaction. Figure 5c shows the influence of the temperature on the conversion of ethylbenzene for $\text{V}_2\text{O}_5/\text{Al}_2\text{O}_3$. It can be seen that a sharp drop takes place at 500 °C and 550 °C. In this case, the cause can be attributed to the coke formation, as reported by Chen et al. [21]. Figure 5d shows a comparison of ethylbenzene consumption for all the catalysts that confirms $\text{MnO}_2\text{-ZrO}_2$ exhibits the best results at a high temperature where coke formation is significant, although $\text{V}_2\text{O}_5/\text{Al}_2\text{O}_3$ is more active for the reaction.

Figure 6 represents the CO_2 consumption after the reaction. It can be seen that CO_2 conversion in the first pulses is higher for $\text{V}_2\text{O}_5/\text{Al}_2\text{O}_3$ at 550 °C than in the other catalysts. It is worth remarking on the positive role that CeO_2 plays in the $\text{V}_2\text{O}_5\text{-CeO}_2/\text{TiO}_2\text{-ZrO}_2$ catalyst for facilitating catalyst oxidation at lower temperatures [29, 30].

Figure 7 shows the overall coke formed during the ethylbenzene reaction in each catalyst test. This is the result of the combustion of the remaining coke with pulses of O_2 . It can be seen that $\text{MnO}_2\text{-ZrO}_2$ and V-TiO_2 significantly generated less coke than the other two catalysts. According to the values presented in Table 2, a lower coke formation was observed in the case of V-TiO_2

than $\text{MnO}_2\text{-ZrO}_2$ (0.068 mmol O_2 / g cat. was necessary to consume for completely removing it). However, $\text{MnO}_2\text{-ZrO}_2$ stability was better, as shown in Figure 5.

Table 3 shows the influence of the catalyst oxidation state on the conversion of ethylbenzene. To carry out the study, $\text{MnO}_2\text{-ZrO}_2$ was selected. The sample called *reduced* was treated with H_2 pulses before the ethylbenzene reaction. For the *partially oxidized* catalyst, the sample was previously reduced with H_2 and later with CO_2 while the *oxidized* catalyst was not treated. The ethylbenzene reaction was carried out sending pulses at two ethylbenzene partial pressures taking into account the vapour pressure of the ethylbenzene saturated in helium that was fed into the reactor. It can be seen that conversion is lower for the reduced catalyst but the partially and completely oxidized catalysts are similar. This proves that the CO_2 oxidation is sufficient to favour ethylbenzene dehydrogenation. After every test reaction, CO_2 pulses were sent to catalyst reoxidation. Finally, O_2 was injected in order to recover the catalyst completely. It was observed that CO_2 consumption is slightly higher when the catalyst is more reduced. This can be due to the acid character of the CO_2 that makes the oxidation of manganese faster when it is reduced with a previous reduction step with hydrogen. Moreover, the CO_2 is able to oxidize a fraction between 17-25 % of the overall oxidation of the catalyst depending on the previous oxidation state. The addition of a sufficient amount of CO_2 is therefore enough to keep the catalyst active for the ethylbenzene reaction operating in a redox mode.

4. Conclusions

Four catalysts selected from the most promising reported in the literature have been tested in order to identify the most suitable one for using in a redox process without deactivation by coke. $\text{V}_2\text{O}_5/\text{Al}_2\text{O}_3$ exhibited the highest coke formation and caused a progressive deactivation in the transient study with ethylbenzene. CO_2 partially oxidizes the catalyst, but not sufficiently in order to regenerate it in a short time. The same performance was obtained for V-TiO_2 but, in this case,

lattice oxygen was not enough to keep the ethylbenzene conversion. The addition of CeO₂ to the V₂O₅-CeO₂/TiO₂-ZrO₂ catalyst facilitates the reduction but the activity for the reaction is low. MnO₂-ZrO₂ showed the best performance with high activity, stability and redox properties. Coke hardly appears at low temperatures and, at 550 °C, it does not affect significantly to the conversion. A study to determine the influence of the oxidation state for this catalyst showed that CO₂ can reoxidize a considerable part of the catalyst. Thus the addition of the appropriate amount of CO₂ can counteract the catalyst deactivation to operate continuously with this reaction.

Acknowledgements

This work has been funded by the Ministry of Education and Science (project CTQ-2010-15568).

References

- [1] F. Cavani, F. Trifirò, *Appl. Catal. A: Gen.* 133 (1995) 219.
- [2] S. Wang, Z.H Zhu, *Energy and Fuels* 18 (4) (2004)1126.
- [3] R. Mallada, M. Menéndez, J. Santamaría, *Appl. Catal. A: Gen.* 231 (1-2) (2002) 109.
- [4] B.M Reddy, S.C. Lee, D.S. Han, S.E. Park, *Appl. Catal. B: Environ.* 87 (3-4) (2009) 230.
- [5] D.R. Burri, K.M. Choi, D.-S. Han, J.-B. Koo, S.-E. Park, *Catal. Today* 115 (2006) 242.
- [6] D.R. Burri, K.M. Choi, D.-S. Han, Sujandi, N. Jiang, A. Burri, S.-E. Park, *Catal. Today* 131 (2008) 173.
- [7] H. Li, Y. Yue, C. Miao, Z. Xie, W. Hua, Z. Gao, *Catal. Commun.* 8 (9) (2007) 1317.
- [8] M.-S. Park, V.P. Vislovskiy, J.-S. Chang, Y.-G. Shul, J. Yoo, S.-E. Park, *Catal. Today* 87 (1-4) (2003) 205.
- [9] I.E. Wachs, *Catal. Today* 100 (1-2) (2005) 79.

- [10] J.C.S. de Araujo, C.B.A. Sousa, A.C. Oliveira, F.N.A. Freire, A.P. Ayala, A.C. Oliveira, *Appl. Catal. A: Gen.* 377 (1-2) (2010) 55.
- [11] L.A. Atanda, R.J. Balasamy, A. Khurshid, A.A.S. Al-Ali, K. Sagata, M. Asamoto, H. Yahiro, K. Nomura, T. Sano, K. Takehira, S.S. Al-Khattaf, *Appl. Catal. A: Gen.* 396 (1-2) (2011) 107.
- [12] R.J. Balasamy, A. Khurshid, A.A.S. Al-Ali, L.A. Atanda, K. Sagata, M. Asamoto, H. Yahiro, K. Nomura, T. Sano, K. Takehira, S.S. Al-Khattaf, *Appl. Catal. A: Gen.* 390 (1-2) (2010) 225.
- [13] R.J. Balasamy, B.B. Tope, A. Khurshid, Al-Ali, A.A.S. L.A. Atanda, K. Sagata, M. Asamoto, H. Yahiro, K. Nomura, T. Sano, K. Takehira, S.S. Al-Khattaf, *Appl. Catal. A: Gen.* 398 (1-2) (2011) 113.
- [14] M. Sugino, H. Shimada, T. Turuda, H. Miura, N. Ikenaga, T. Suzuki, *Appl. Catal. A: Gen.* 121 (1) (1995) 125.
- [15] A.H. de Morais Batista, F.F. de Sousa, S.B. Honorato, A.P. Ayala, J.M. Filho, F.W. de Sousa, A.N. Pinheiro, J.C.S. de Araujo, R.F. Nascimento, A. Valentini, A.C. Oliveira, *J. Mol. Catal. A: Chem.* 315 (2010) 86.
- [16] O.V. Krylov, A.K. Mamedov, S.R. Mirzabekova, *Catal. Today* 24 (3) (1995) 371.
- [17] Y. Sakurai, T. Suzaki, N. O. Ikenaga, T. Suzuki, *Appl. Catal. A: Gen.* 192 (2000) 281.
- [18] J.-S. Chang, D.-Y. Hong, V. P. Vislovskiy, S.-E. Park, *Catal. Surv. Asia* 11 (2007) 59.
- [19] A.L. Sun, Z.F. Qin, S.W. Chen, J.G. Wang, *J. Mol. Catal. A: Chem.* 210 (2004) 189.
- [20] V.P. Vislovskiy, J.S. Chang, M.S. Park, S.E. Park, *Catal. Commun.* (3) (2002) 227.
- [21] S. Chen, Z. Quin, X. Xu, J. Wang, *Appl. Catal. A: Gen.* 302 (2) (2006) 185.
- [22] B. Xiang, Ch Yu, H. Xu, W. Li, *Catal. Lett.* 125 (2008) 90.
- [23] Y. Qiao, Ch. Miao, Y. Yue, Z. Xie, W. Yang, W. Hua, Z. Gao, *Micropor. Mesopor. Mat.* 119 (2009) 150.

- [24] N. Jiang, D.S. Han, S.E. Park, *Catal. Today* 141 (2009) 344.
- [25] W. Li, X. Li, J. Feng, *Catal. Lett.* 130 (2009) 575.
- [26] B.M. Reddy, D.-S. Han, N. Jiang, S.-E. Park, *Catal. Surv. Asia* 12 (2008) 56.
- [27] J. Herguido, M. Menéndez, J. Santamaría, *Catal. Today* 100 (1-2) (2005) 181.
- [28] A. Dinse, B. Frank, C. Hess, D. Habel, R. Schomäcker, *J. Mol. Catal. A: Chem.* 289 (2008) 28.
- [29] W. Daniell, A. Ponchel, S. Kuba, F. Anderle, T. Weingand, D.H. Gregory, H. Knözinger, *Top. Catal.* 20 (2002) 65.
- [30] T. Feng, J.M. Vohs, *J. Catal.* 221 (2004) 619.
- [31] J.-N. Park, J. Noh, J.-S. Chang, S.-E. Park, *Catal. Lett.* 65 (2000) 75.

Figure Captions

Figure 1: Experimental setup for pulse experiments.

Figure 2: XRD patterns for fresh and used catalyst. a) V_2O_5/Al_2O_3 : (\star) γ - Al_2O_3 ; b) MnO_2-ZrO_2 : (\circ) ZrO_2 , (\bullet) MnO_2 ; c) $V-TiO_2$: (Δ) anatase, (\blacktriangle) rutile; d) $V_2O_5-CeO_2/TiO_2-ZrO_2$: (\square) ZrV_2O_7 , (\blacksquare) $CeVO_4$.

Figure 3: a) H_2 conversion in the reduction step for every pulse at $550^\circ C$, b) H_2 consumption for the catalysts studied.

Figure 4: CO_2 conversion in the oxidation step for every pulse at $550^\circ C$, b) CO_2 consumption for the catalysts studied.

Figure 5: Ethylbenzene conversion in the reaction step for every pulse at $550^\circ C$, b) ethylbenzene conversion for MnO_2-ZrO_2 catalyst at different temperatures, c) ethylbenzene conversion for V_2O_5/Al_2O_3 catalyst at different temperatures, d) ethylbenzene consumption for the catalysts studied.

Figure 6: CO_2 conversion in the reoxidation step for every pulse at $550^\circ C$, b) CO_2 consumption for the catalysts studied.

Figure 7: Coke removed for the catalysts studied in combustion step.

Table 1: BET surface area values of the catalysts (m²/g).

	Fresh	Used
V ₂ O ₅ /Al ₂ O ₃	137	98
MnO ₂ -ZrO ₂	64	56
V-TiO ₂	5.7	4.9
V ₂ O ₅ -CeO ₂ /TiO ₂ -ZrO ₂	76	75

Table 2: Catalyst oxidation with CO₂ and oxidation/ combustion with O₂ at 550°C

	Catalyst			
	V ₂ O ₅ /Al ₂ O ₃	MnO ₂ -ZrO ₂	V-TiO ₂	V ₂ O ₅ -CeO ₂ /TiO ₂ -ZrO ₂
mmol CO ₂ / g cat. (catalyst oxidation)	0.16	0.064	0.094	0.128
mmol O ₂ / g cat. (catalyst oxidation)	0.67	0.363	0.352	0.250
mmol O ₂ / g cat. (coke combustion)	1.03	0.157	0.068	0.410

Table 3: Effect of previous catalyst oxidation state on ethylbenzene conversion and CO₂ and O₂ consumption for MnO₂-ZrO₂ catalyst at 550°C.

	Catalyst					
	Reduced		Partially oxidized		Oxidized	
	P _V =2.44%	P _V =5.05%	P _V =2.44%	P _V =5.05%	P _V =2.44%	P _V =5.05%
Conversion ethylbenzene (%)	73.73	69.87	82.95	95.98	82.95	95.31
mmol CO ₂ / g cat. (catalyst oxidation)	0.059	0.083	0.057	0.081	0.055	0.066
mmol O ₂ / g cat. (catalyst oxidation)	0.215	0.254	0.217	0.333	0.264	0.325
mmol O ₂ / g cat. (coke combustion)	0.101	0.114	0.105	0.153	0.130	0.153

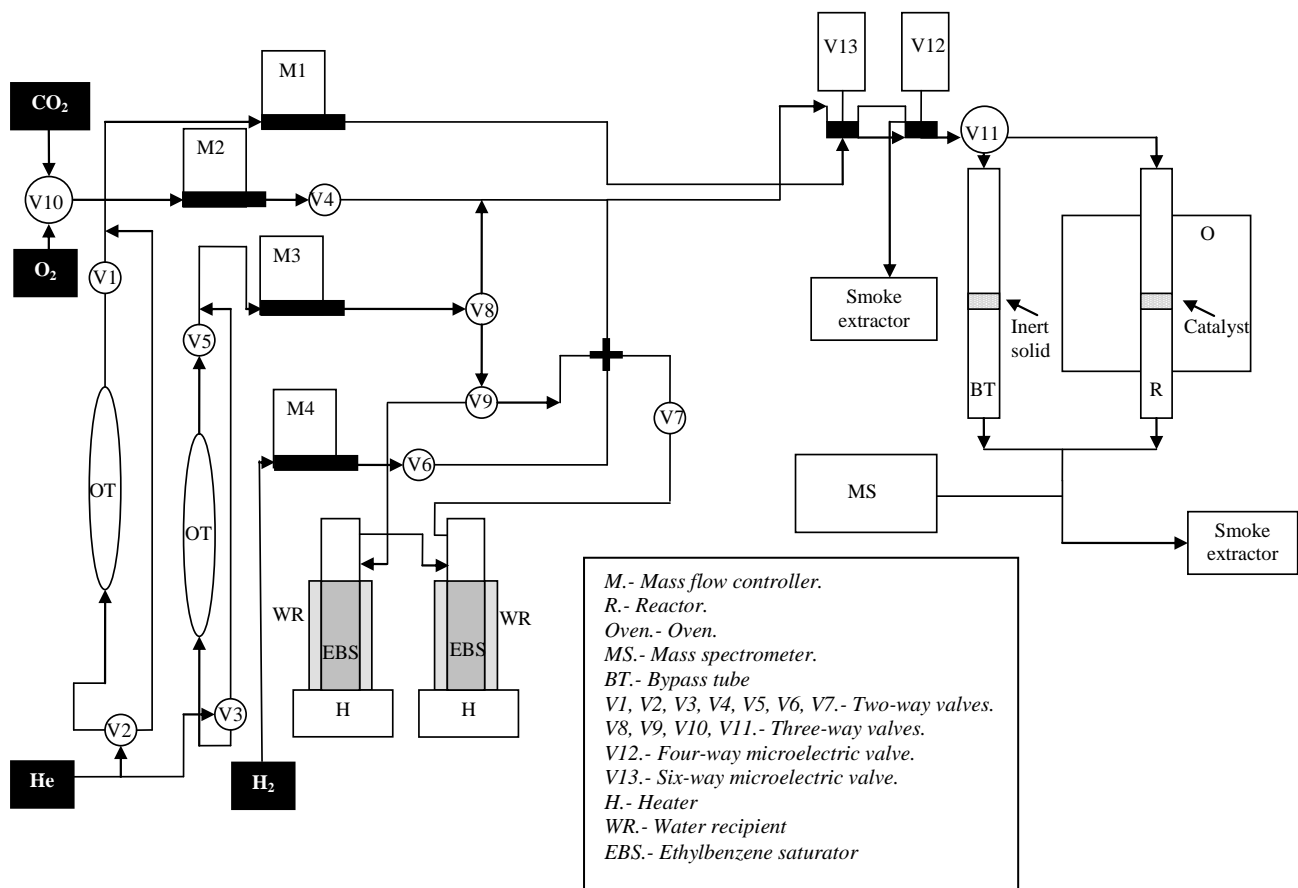


Figure 1

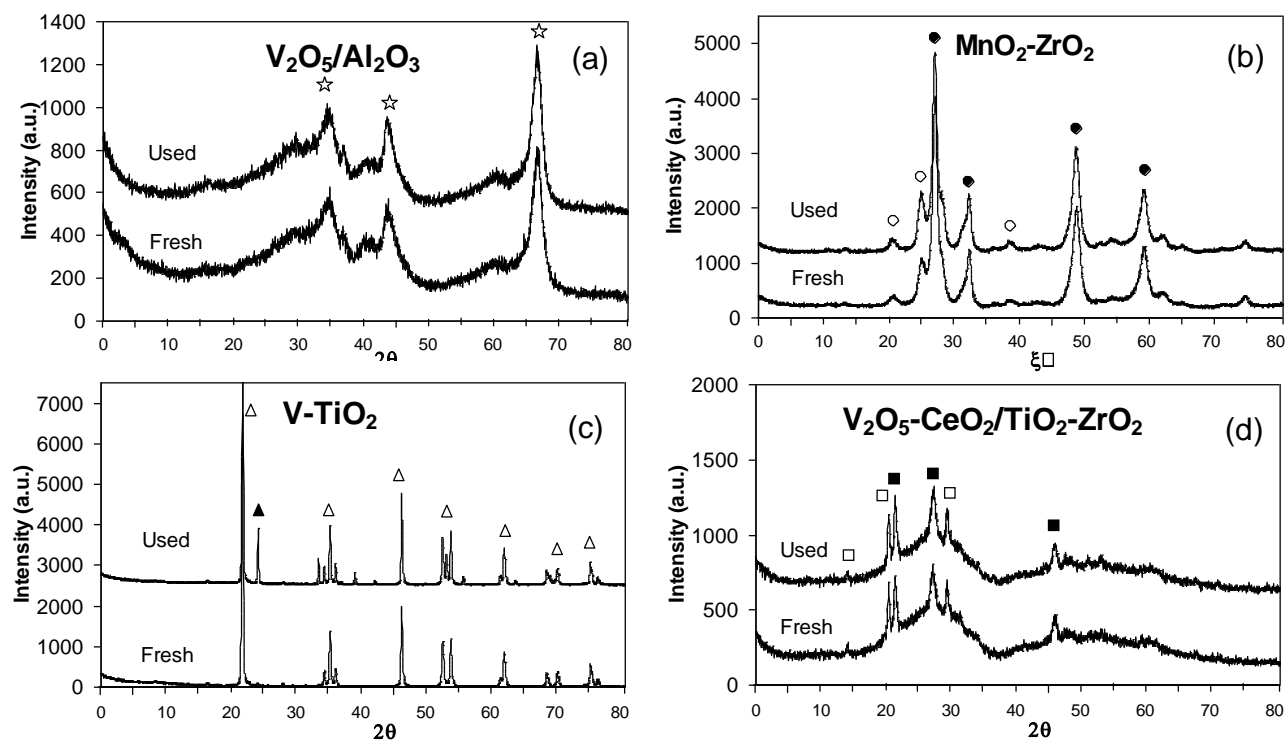


Figure 2

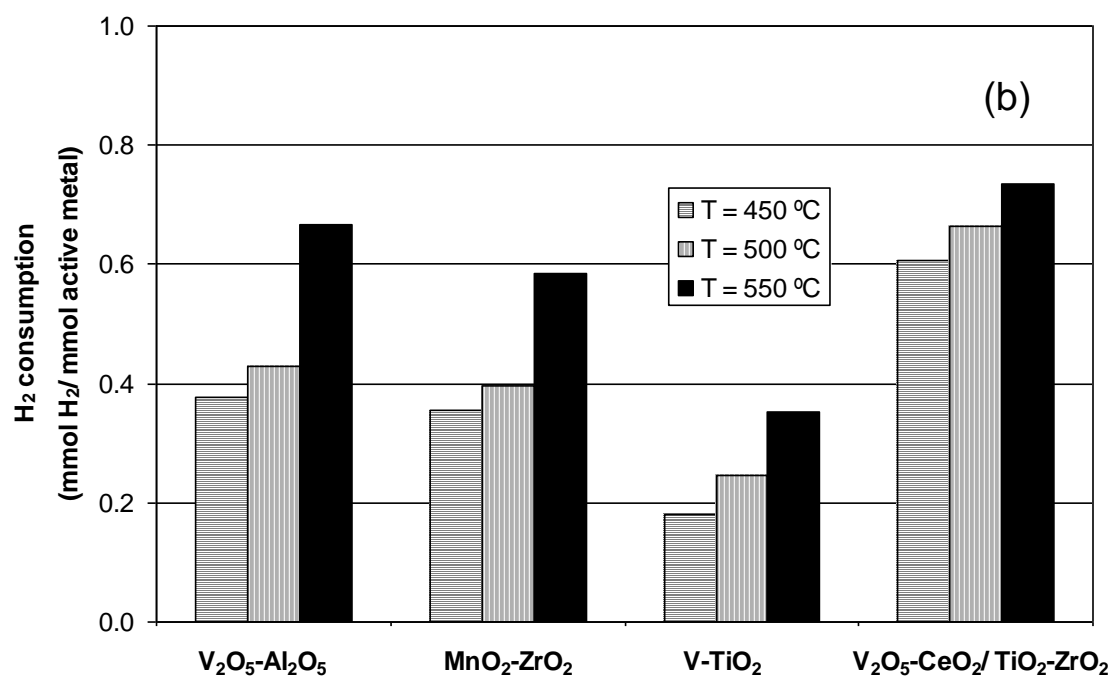
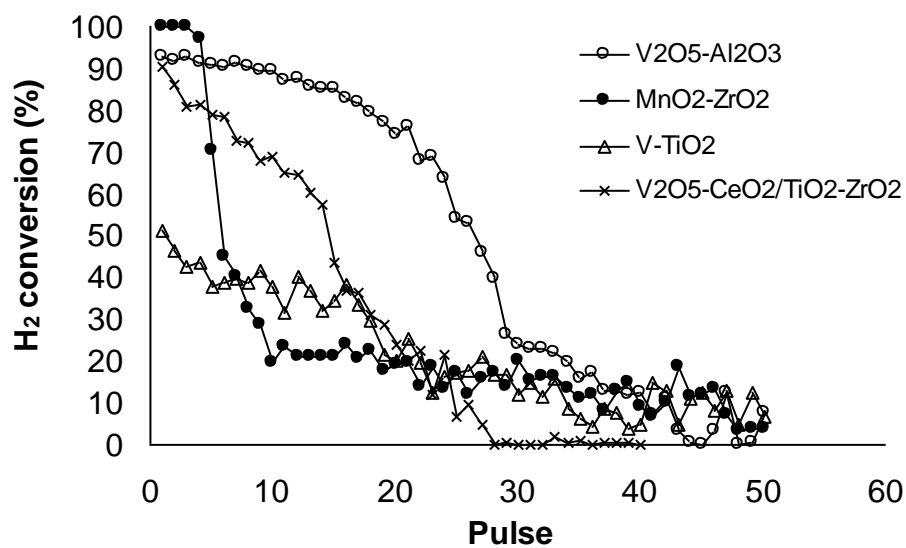


Figure 3

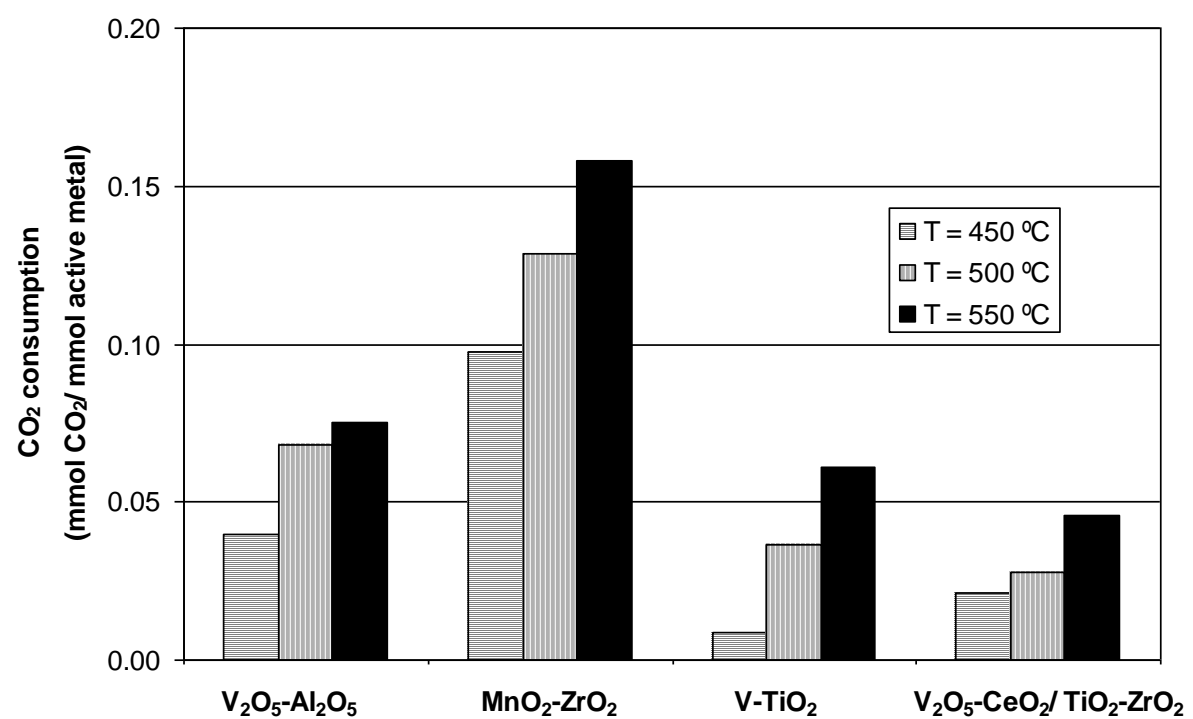
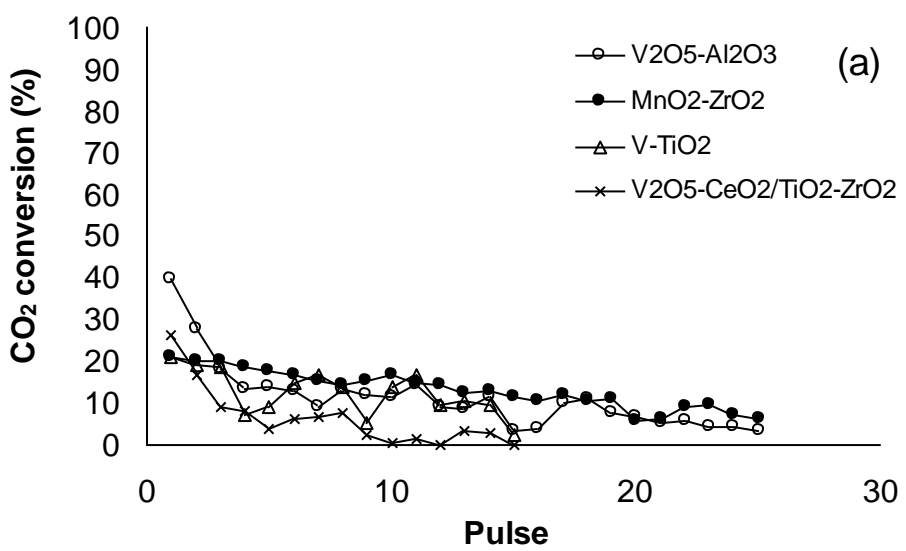
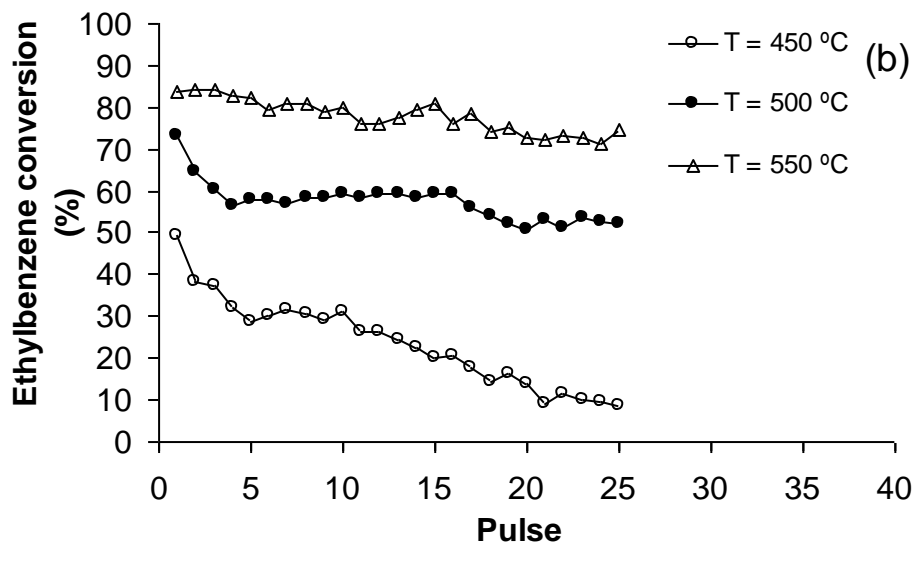
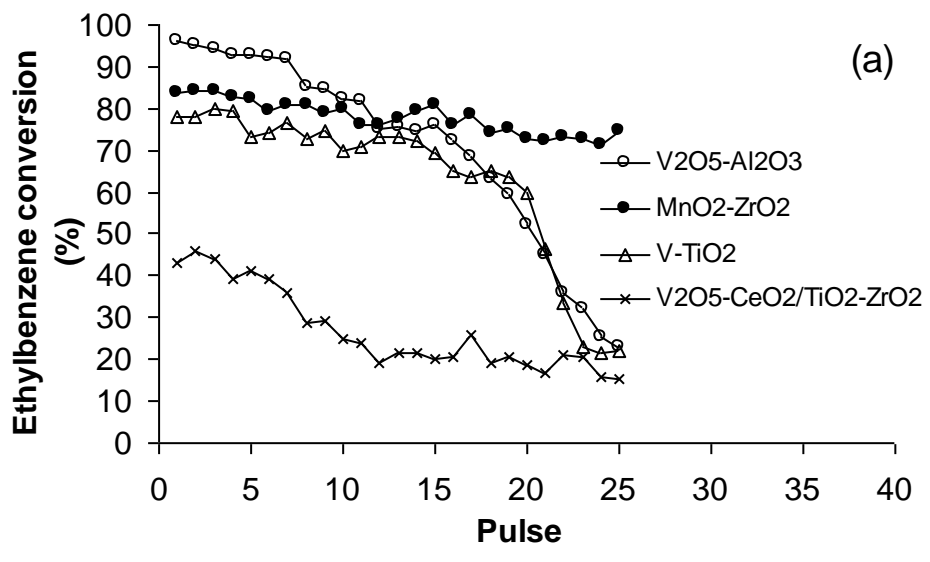


Figure 4

Figure



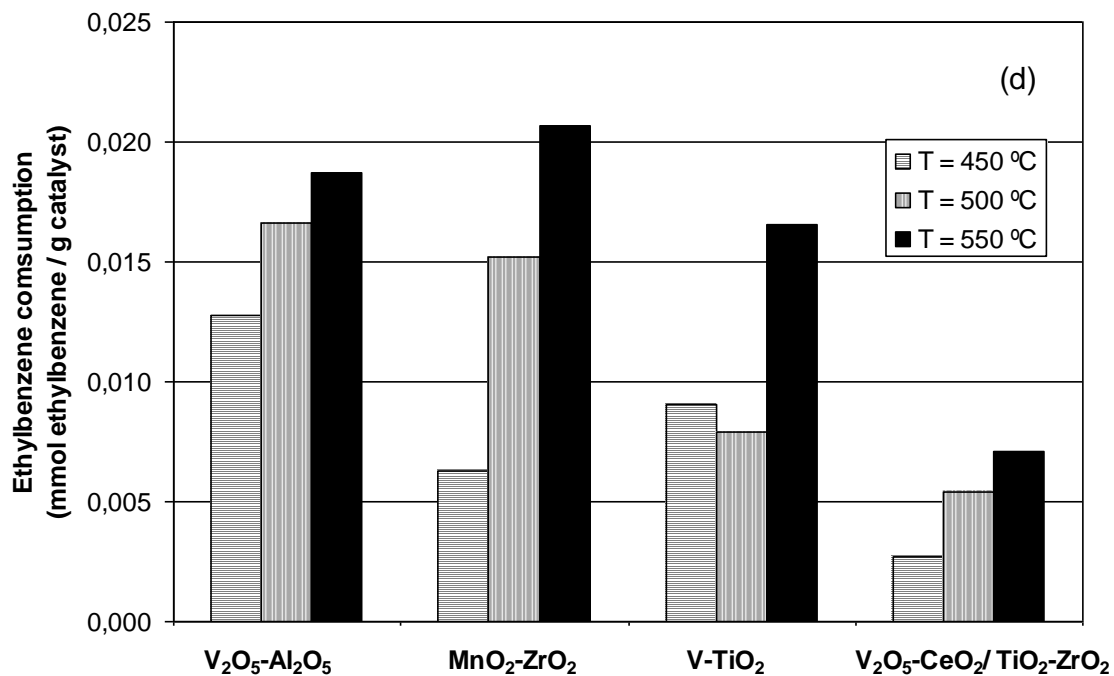
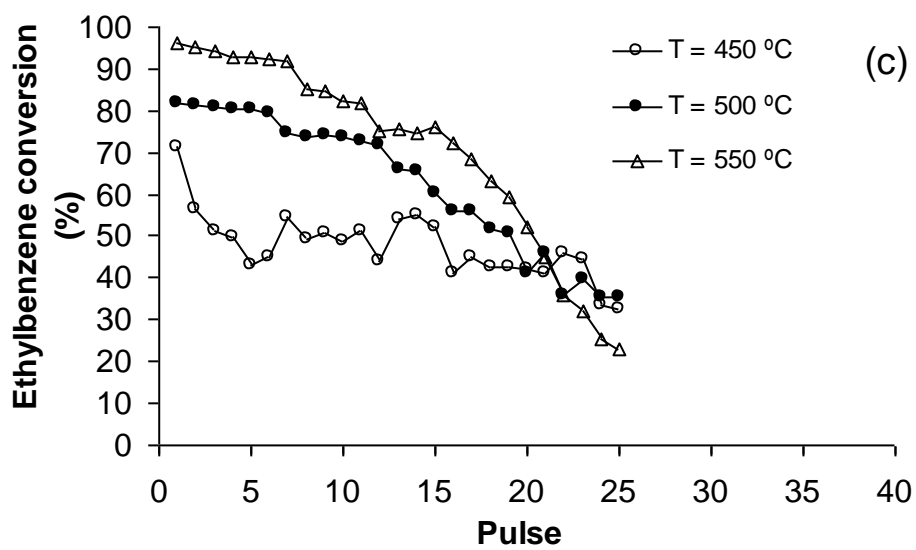


Figure 5

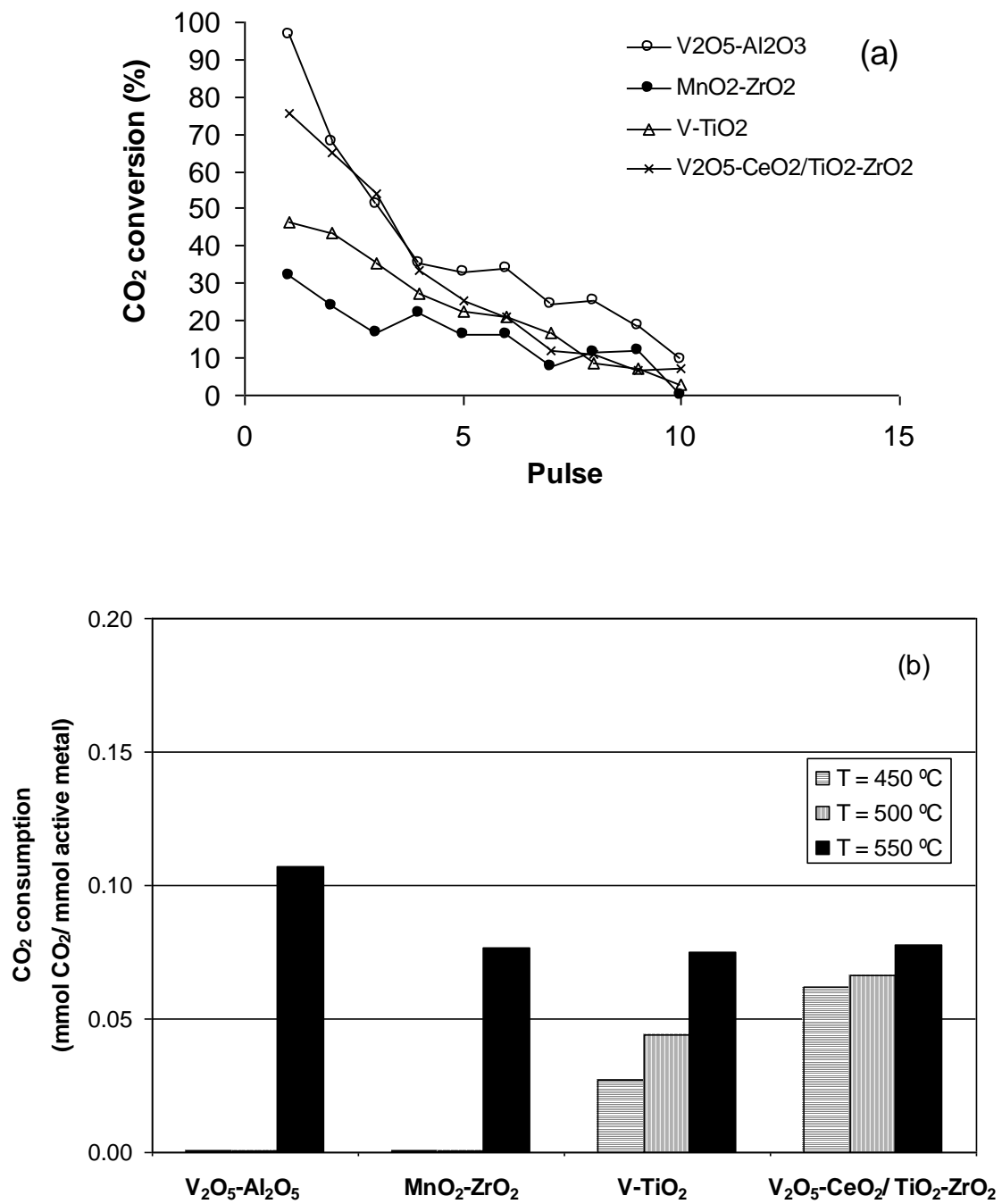


Figure 6

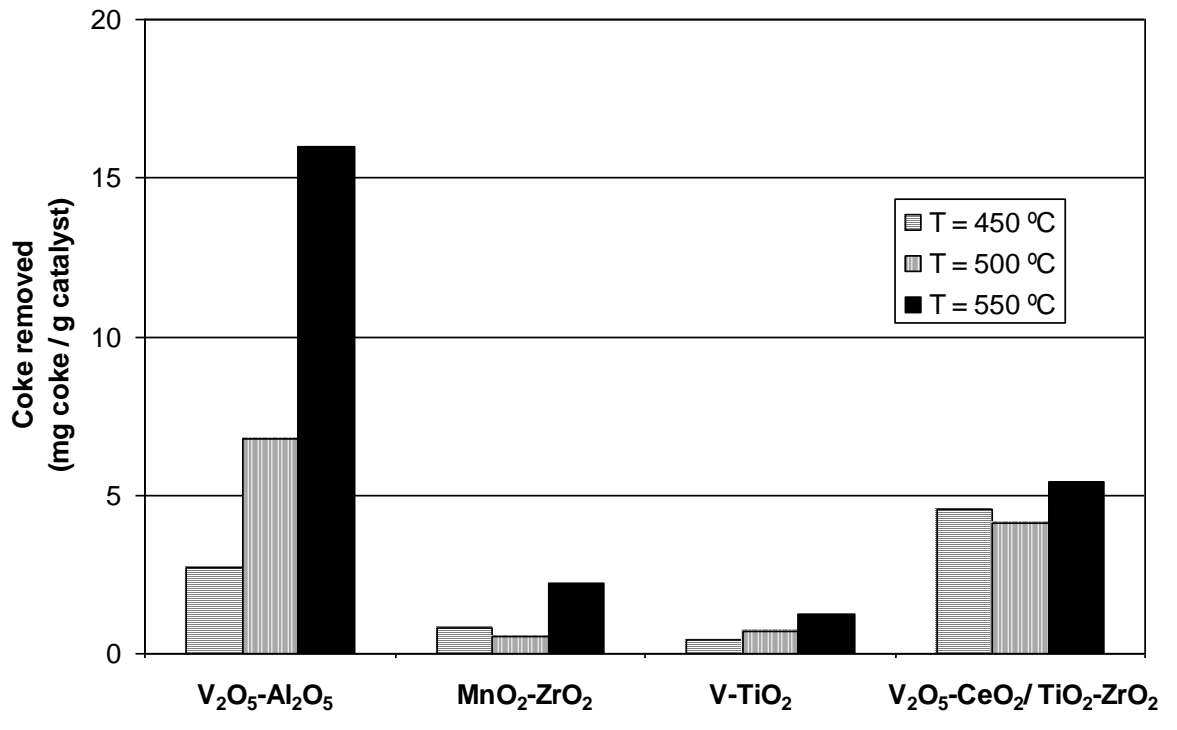


Figure 7